JOURNAL OF SOLID STATE CHEMISTRY 25, 85–99 (1978)

The Crystal Structure of the Cu^+ Ion Conductor, $(C_5H_5NH)_2Cu_5Br_7$*

L. Y. Y. CHAN† AND S. GELLER

Department of Electrical Engineering, University of Colorado, Boulder, Colorado 80309

AND P. M. SKARSTAD‡

Medtronic, Inc., 3055 Old Highway Eight, Minneapolis, Minnesota 55440

Received September 19, 1977

$(C_5H_5NH)_2Cu_5Br_7$, in which $(C_5H_5NH)^+$ is the pyridinium ion, belongs to space group $P2_12_12_1$ with $Z = 4$ and $a = 13.09 \pm 0.03$ Å, $b = 14.04 \pm 0.03$ Å, $c = 11.78 \pm 0.02$ Å. The 20 Cu^+ ions are distributed non-uniformly over 52 tetrahedral sites. The bromide tetrahedra share faces in such a manner that undulating channels are formed in the [100] and [010] directions, and right- and left-handed helical channels are formed in the *c*-direction. The channels are interconnected, thereby forming a three-dimensional solid electrolyte. A detailed examination of the conduction pathways and of Cu^+ ion site occupancies leads to the predictions that σ_2 ($\|b$) should be somewhat greater than σ_1 ($\|a$) but σ_3 ($\|c$) should be substantially less than σ_1. (σ_i is the specific conductivity in the *i*th direction.) The ratio of available sites to current carriers and the percentage of unit cell volume attributable to the conduction pathways are both rather low and the *average* conductivity is rather high relative to AgI-based solid electrolytes.

Introduction

Several crystal structures of solid electrolytes in which the Ag^+ ion is the current carrier and mostly iodide ions form the "rigid framework" have been determined (*1–4*). The relation of these structures to the conductivity of the crystals has been discussed in some detail (*1–11*). Among the more important features of the AgI-based solid electrolyte structures is the network of pathways formed as a result of the face-sharing of the iodide ion polyhedra[1] and the substantial excess of sites available to the Ag^+ ions over Ag^+ ions available as current carriers. The networks are different in detail in different structures; as might be intuitively expected, those crystals with simpler three-dimensional networks have the higher bulk conductivities. In an anisotropic solid electrolyte in which the network of pathways is three-dimensional, the highest conductivity is in the direction of the simplest pathways. Solid electrolytes in which the conductivity is not three-dimensional generally have low conductivities (see for example, Refs.

* Supported by the National Science Foundation under Grants DMR Nos. 72-03271-A01 and 77-11378-A01.

† Present address: Department of Biochemistry, University of Toronto, Toronto, Ontario M5S 1A8, Canada.

‡ Part of whose contribution was a result of work performed at the National Bureau of Standards, Washington, D.C.

[1] In $Ag_{26}I_{18}W_4O_{16}$ (*4*), the oxygen atoms of the $(W_4O_{16})^{8-}$ ion are also involved in the formation of the polyhedra in the conduction network. This is expected to be the case in other solid electrolytes that involve complex oxide anions.

0022–4596/78/0251–0085$02.00/0

(*3*, *6–9*)). For discussion of other features of halogenide solid electrolytes, see Refs. (*2–12*).

A very large number of solid electrolytes based on AgI has been reported (*12–16*); however, there are so far not many solid electrolytes in which the Cu^+ ion is the current carrier. It is not really clear why this is so, but it must be related, at least to some extent, to the sizes of the current carriers relative to the sizes and polarizabilities of the halide ions.

In this paper, we report the first structure determination of a double salt in which the Cu^+ ion is the current carrier. The formula of this solid electrolyte is $(C_5H_5NH)_2Cu_5Br_7$ or $Py_2Cu_5Br_7$, in which Py^+ is the pyridinium ion. This solid electrolyte was first reported by Sammells *et al.* (*17*). Crystals of the material have been grown (*18*) by one of us (P.M.S.) by means of a modified Bridgman technique.

Relative to methodology, this is the first of the solid electrolyte structures that we have determined by direct methods.

Experimental

Crystals of $Py_2Cu_5Br_7$ are sensitive to oxygen; therefore the handling of the crystals was done in a dry N_2 atmosphere in a drybox. Initially, X-ray photographs of a crystal fragment coated with epoxy cement were taken on a Buerger precession camera; these photographs were the $0kl$–$4kl$ and the $h0l$ levels. The data confirmed the reported (*17*, *18*) orthorhombic space group, $P2_12_12_1(D_2^4)$; that is, reflections $h00$, $0k0$, and $00l$ were present only when h, k, l were even. The lattice constants obtained from these photographs are $a = 13.09 \pm 0.03$ Å, $b = 14.04 \pm 0.03$ Å, and $c = 11.78 \pm 0.02$ Å. The formula weight of $Py_2Cu_5Br_7$ is 1037.50; the unit cell volume is 2165 Å^3. The unit cell can contain only multiples of 4 $Py_2Cu_5Br_7$ in the most probable space group $P2_12_12_1$. With one multiple, i.e., 4 $Py_2Cu_5Br_7$, the calculated X-ray density is 3.18 g cm^{-3}, which is in good agreement with the value 3.178 g cm^{-3} reported (*17*) as the "observed" density.[2]

A crystal was ground to a sphere of radius 0.096 mm with a sphere grinder (*19*) similar to that described by Schuyff and Hulscher (*20*). (Dry N_2 was used in the grinding process.) The spherical crystal was coated with epoxy cement, which was allowed to dry. The coated crystal was then put into a Lindeman capillary of 0.3-mm diam, 0.01-mm wall thickness. After the crystal was located near the closed end of the tube, a very small amount of epoxy cement was introduced to cause the crystal to remain attached to the wall of the capillary. The capillary was sealed off and mounted on a goniometer head.

The crystal was aligned with the a-axis as rotation axis. Intensities of the independent reflections in the range $10° \leqslant 2\theta \leqslant 45°$ (Zr-filtered, Mo$K\alpha$ radiation), were collected with a Buerger–Supper single-crystal diffractometer automated by a Nova 1200 computer. Each reciprocal lattice point was scanned at the rate of 1.5°/min over the range (1.5 + 0.7 Lp), where Lp is the Lorentz–polarization–Tunnel factor. The maximum scan range for any peak was limited to 5°. Background counts were taken at the beginning and at the end of the scan interval at one-fourth the scan time of each scan. Intensities of data beyond $2\theta = 45°$ were not significant. The total number of independent reflections measured was 1591, of which 684 were below the 70-count threshold.

The linear absorption coefficient, μ, of $Py_2Cu_5Br_7$ for Mo$K\alpha$ radiation is 186.8 cm^{-1}, from which, for $R = 0.096$ mm, $\mu R = 1.80$. It should be noted that this absorption is high, and the scattering matter in the crystal low, relative to the AgI-based solid electrolytes. That is, the individual intensities for this crystal tended to be relatively low overall. The Nova computer does some of the data processing, applying the background, absorption, and Lorentz–polarization–Tunnel corrections and

[2] Although not so explicitly stated in Ref. (*17*), the measured density was obtained by the flotation method (private communication from B. B. Owens).

giving, on paper tape, the relative squares of the structure amplitudes.

Determination and Refinement of the Structure

In the space group $P2_12_12_1(D_2^4)$, there are only the fourfold general positions. Thus in crystals of $Py_2Cu_5Br_7$, the formula unit is the asymmetric unit.

The structure was solved by direct methods with the FAMEB (*21*) and MULTANB programs (*22*); *E*-maps were calculated with FORDAPB (*23*). The trial model indicated that the seven independent Br^- ions were at the apices of a pentagonal bipyramid. A structure factor calculation[3] involving only the Br^- ions gave $R = 0.44$ ($R = \Sigma| |F_o| - |F_c| |/\Sigma|F_o|$). Two cycles of least-squares refinement with isotropic thermal parameters reduced R to 0.34.

The pentagonal bipyramid contains 5 face-sharing tetrahedra. A model of the four pentagonal bipyramids arranged in the unit cell showed that there were 8 more independent face-sharing tetrahedra connecting the bipyramids, thus giving a total of 13 independent face-sharing anion tetrahedra. Initially, the 5 Cu^+ ions per formula unit were assumed to be equally distributed over the 13 tetrahedral sites. Several least-squares cycles in which the site occupancies of the Cu^+ ions were varied brought R to 0.20. In these calculations, positional parameters were varied, but not all at the same time. The thermal parameters in these cycles were all taken as isotropic.

The Br^- ions and the Cu^+ ions in the three most populated ($m > 0.80$)[4] sites were assigned anisotropic thermal parameters; the remainder of the Cu^+ ions were still assigned isotropic thermal parameters of 7.5 Å^2. Further least-squares cycles reduced R to 0.12.

[3] All least-squares and structure factor calculations were carried out with NUCLS 5 (*24*).

[4] m = number of atoms in particular set of positions/number of equipoints in set of general positions.

The next step was to find the location of the Py^+ ions. The surroundings of the Py^+ ions in the structures of PyI (*25*), $PyAg_5I_6$ (*2*), and $Py_5Ag_{18}I_{23}$ (*3*) were studied to see whether any resemblance could be found to Br^- ion arrangements about as yet unfilled space in the model. This gave only some notion as to what to look for, but it was clear that the arrangement of Br^- ions surrounding the Py^+ ions was not the same as the arrangement of iodide ions surrounding the Py^+ ions in the iodide compounds. An approximately planar array of six Br^- ions arranged hexagonally was seen. One Py^+, Py1, was estimated to lie approximately parallel to this hexagon; this also linked Py1 to seven more Br^- ions on the side opposite that of the hexagon. Calculation of the 119 structure amplitudes, including the contribution from Py1,[5] with the largest $\Delta = ||F_o| - |F_c||$ showed significant improvement, i.e., a decrease of the average Δ. Several least-squares cycles followed with Py1 included, and anisotropic thermal parameters for two more Cu^+ ions. R was thereby reduced to 0.09.

The second Py^+ ion, Py2, could be seen to fit on the side of the Br^- ion hexagon opposite that of Py1, but its orientation was uncertain. One hundred twenty structure amplitudes with $(\sin\theta)/\lambda < 0.3$ and with the largest Δ's were used to calculate a difference Fourier map which gave the orientation of Py2.

Least-squares calculations were continued. The imaginary parts of the atomic scattering factors (*26*) were introduced and one enantiomorph was found to give significantly better agreement than the other ($R = 0.076$ vs 0.083). (The final parameters listed in Table I are for the more probable enantiomorph.)

Because of the rigid group refinement, the C and N atoms in the Py^+ ion were not distinguished. With regard to the (independent) Cu^+ ion sites, only five had fractional occupancies $\geqslant 0.70$. The remaining eight had

[5] In all calculations, each Py^+ ion was treated as a rigid body benzene ring with a temperature factor 7.8 Å^2 for each atom of the ring.

TABLE I

PARAMETERS AND STANDARD ERRORS OF Cu^+ AND Br^- IONS IN $Py_2Cu_5Br_7$

Ion	m[a]	x	y	z	β_{11}[b]	β_{22}	β_{33}	β_{12}	β_{13}	β_{23}
Br1	1.0	0.3672(4)	0.0704(4)	-0.2293(5)	26(3)	47(3)	119(7)	2(3)	- 7(4)	17(4)
Br2	1.0	0.4283(4)	0.2388(4)	0.0346(5)	19(3)	54(4)	87(6)	16(3)	2(4)	5(4)
Br3	1.0	0.3825(4)	0.5235(4)	-0.0396(6)	29(3)	64(4)	117(6)	8(3)	6(4)	6(5)
Br4	1.0	0.6664(4)	0.1248(4)	-0.1409(5)	41(3)	57(4)	87(6)	7(3)	- 3(4)	- 1(4)
Br5	1.0	0.6738(4)	0.4058(4)	-0.0257(6)	18(3)	76(4)	107(6)	6(3)	29(4)	26(4)
Br6	1.0	0.1899(4)	0.3146(4)	-0.1947(5)	34(3)	63(4)	104(6)	- 2(3)	-12(4)	-23(4)
Br7	1.0	0.4833(4)	0.3316(4)	-0.2909(6)	33(3)	62(4)	136(8)	- 8(3)	16(5)	- 6(5)
Cu1	0.80	0.4921(7)	0.1904(9)	-0.1746(10)	43(6)	117(9)	148(13)	-39(6)	10(7)	-40(9)
Cu2	0.11	0.534	0.138	-0.280	*					
Cu3	0.14	0.542	0.013	-0.261	*					
Cu4	0.70	0.4708(11)	-0.0481(13)	0.6440(13)	94(11)	145(14)	173(18)	- 5(10)	- 2(12)	-28(14)
Cu5	0.13	0.492	0.375	-0.080	*					
Cu6	0.10	0.564	0.276	-0.106	*					
Cu7	0.89	0.6196(7)	0.2385(7)	0.0009(10)	41(5)	71(6)	172(12)	- 2(5)	- 7(7)	27(7)
Cu8	0.07	0.741	0.243	-0.002	*					
Cu9	0.81	0.7907(7)	0.3154(8)	0.1009(9)	52(7)	71(7)	128(11)	- 3(5)	1(7)	22(7)
Cu10	0.18	0.367	0.240	-0.170	*					
Cu11	0.70	0.3473(11)	0.3676(11)	-0.1101(13)	95(11)	125(12)	170(17)	-15(10)	20(11)	13(12)
Cu12	0.28	0.292	0.363	-0.015	*					
Cu13	0.10	0.347	0.449	-0.220	*					

[a] m = multipler (see text).

[b] The form of the temperature factor is $T = \exp[-(h^2\beta_{11} + k^2\beta_{22} + l^2\beta_{33} + 2hk\beta_{12} + 2hl\beta_{13} + 2kl\beta_{23})]$; β values $\times 10^4$.

* A constant isotropic thermal parameters $B = 7.5$ Å^2 was assigned to each of these Cu^+ sites.

fractional occupancies $\leqslant 0.28$; in most of the least-squares cycles (especially the last 10 or so) the positional and thermal parameters of these sites were held constant. However, their positions were adjusted after each computer run to give reasonable Cu–Br and Cu–Cu distances. In both cases, i.e., of the Py^+ ions and of Cu^+ ion sites, it seemed improbable that the data would allow individual parameter refinement.

In the antepenultimate cycle, the refinement of all the Cu^+ ion multipliers gave a total of 4.76 Cu^+ ions per formula unit, with individual standard errors of 0.016. The 0.24 Cu^+ ion was distributed among the 10 sites with lowest occupancy. The multipliers were held constant in the last two cycles.

The final R value is 0.076 for 913 observed structure amplitudes. Among the 684 unobserved structure amplitudes, 29 gave calculated values higher than threshold. Including the Δ's for these in the numerator of R, the resulting value is 0.078. The standard error of an observation of unit weight is 1.11.

In the calculations, the data were weighted according to

$$\begin{aligned} F < 100, &\qquad \sigma = 15 - 0.1F, \\ 100 \leqslant F < 150, &\qquad \sigma = 0.05F, \\ F \geqslant 150, &\qquad \sigma = \exp(F/74.45), \\ &\qquad w = 1/\sigma^2. \end{aligned}$$

The atomic scattering factors for Cu^+, Br^-, and C were those of Cromer and Mann (*27*). The real and imaginary parts of the anomalous dispersion were those given by Cromer and Liberman (*26*). A table listing the observed and calculated structure amplitudes is available.[6] Table I lists final parameters and standard errors for the Br^- ions and Cu^+ ion sites. Table II lists the final parameters of the rigid groups representing the pyridinium rings.

[6] See NAPS document No. 03217 for 9 pages of supplementary material. Order from ASIS/NAPS, Microfiche Publications, 440 Park Avenue South, New York, N.Y. 10016. Remit in advance $3.00 for microfiche copy or for photocopy, $5.00 up to 20 pages plus 25¢ for each additional page. All orders must be prepaid. Foreign orders add $5.00 for postage and handling.

Interionic Distances

Table III gives detailed information on each of the Cu^+ ion sites: its fractional occupancy, the associated Br–Br distances[7] and their average, the Cu–Br distances and their average, the number of nearest-neighbor Cu^+ ion sites, the distances thereto and their average, and the volume of the tetrahedron. Standard errors of Br–Br distances are between 0.008 and 0.010 Å. Standard errors of Cu–Br distances involving the sites with fractional occupancy $\geqslant 0.70$ are 0.01 Å for Cu1, 7, 9 and 0.02 Å for Cu4 and Cu11. Because of the way in which the positions of the other Cu^+ ion sites were obtained (see above), there is no estimate of the error of the other Cu–Br distances. This is also the case for Cu–Cu distances.

Table IV lists the number of nearest Br^- ion neighbors of each Br^- ion and their average distance. A table listing distances between the atoms in the Py^+ ions and neighboring atoms will be sent to those requesting the F_c vs F_o tables from Microfiche Publications, Inc. (see footnote 6).

It is of interest to compare the Br–Br, Cu–Br, and Cu–Cu distances in $Py_2Cu_5Br_7$ with those in α- and γ-CuBr. The β–α transition of CuBr occurs at 470°C (*30*); the lattice constant of α-CuBr is 4.601 Å at 485°C (*31*) (see also (*32*)). This phase has Br^- ions at corners and body center of the unit cell and Cu^+ ions distributed over the 12 tetrahedral sites only (*31*); α-CuBr is the solid electrolyte phase (*33*). In α-CuBr at 485°C, the Cu–Br distances are 2.57 Å. There are two different Br–Br distances 3.98 Å and 4.60 Å, four of the former connecting corners to body centers and two of the latter connecting corner to

[7] Distances in Table III were calculated with the program ORFFEC (*28*). However, throughout this study, the ORTEP (*29*) program was used to check distances; ORTEP was also used to make all the figures.

TABLE II

DERIVED PARAMETERS FOR THE RIGID GROUP ATOMS OF $Py_2Cu_5Br_7$

Atom	x	y	z	B (Å^2)	Atom	x	y	z	B (Å^2)
*A*1	0.547(4)	0.403(3)	0.254(4)	7.8	*A*2	0.290(4)	0.167(4)	0.288(3)	7.8
*B*1	0.441(4)	0.413(3)	0.255(4)	7.8	*B*2	0.392(3)	0.157(4)	0.317(4)	7.8
*C*1	0.392(3)	0.448(4)	0.351(5)	7.8	*C*2	0.425(3)	0.178(4)	0.426(4)	7.8
*D*1	0.450(4)	0.474(3)	0.446(4)	7.8	*D*2	0.355(4)	0.211(4)	0.507(3)	7.8
*E*1	0.555(4)	0.464(4)	0.444(4)	7.8	*E*2	0.253(3)	0.221(4)	0.477(4)	7.8
*F*1	0.604(3)	0.428(4)	0.348(5)	7.8	*F*2	0.220(3)	0.200(4)	0.368(4)	7.8

	Rigid group parameters					
Group	x_c[a]	y_c	z_c	δ[b]	ε	η
Py1	0.498(3)	0.4383(21)	0.350(3)	1.67(4)	2.67(3)	1.15(3)
Py2	0.323(3)	0.189(3)	0.397(3)	−1.83(3)	2.89(3)	1.87(3)

[a] x_c, y_c, and z_c are the fractional coordinates of the origin of the rigid group.

[b] The rigid group orientation angles δ, ε, and η (radians) have been defined previously: S. J. La Placa and J. A. Ibers, *Acta Crystallogr.* **18**, 511 (1965).

corner and body center to body center; the weighted average is 4.19 Å. The Cu(site)–Cu(site) distance is 1.63 Å.

The γ-CuBr is the ZnS-type phase. Assuming the correct lattice constant to be that given by Swanson *et al.* (*34*), 5.6905 Å at 26°C, the Br–Br and Cu–Br distances are 4.02 and 2.46 Å, respectively.

In $Py_2Cu_5Br_7$, the range of Br–Br distances is 3.735–5.124 Å (Table III). This range includes only Br–Br edges of tetrahedra. Two distances, 5.077 and 5.124 Å, in this range seem rather large especially relative to I–I distances in the AgI-based solid electrolytes. At the low end, 3.735 Å is reasonable relative to I–I distances in iodide tetrahedra; for example, in $Py_5Ag_{13}I_{23}$ (*3*), there is an I–I distance of 3.984 Å, and an I–I distance of 4.03 Å in $Ag_{26}I_{18}W_4O_{16}$ (*4*). The range of the average of six Br–Br distances in the tetrahedra (Table III), 4.051–4.389 Å, seems reasonable, though relatively broader than has been observed in the AgI-based solid electrolytes. The overall average of the Br–Br distances in the tetrahedra is 4.148 Å, which is rather close to the average Br–Br distance in α-CuBr at 485°C.

The Cu–Br distances, including those adjusted as described earlier, have the range 2.41–2.96 Å. This is reasonable relative to the Ag–I distances in the AgI-based solid electrolytes. Some of the Cu–Cu nearest-neighbor distances may appear to be rather short but they are all reasonable relative to Ag–Ag nearest-neighbor distances in AgI-based solid electrolytes. The overall average of the Cu–Br distances (per tetrahedron) is 2.55 Å and that of the Cu–Cu distances is 1.67 Å; these are close to the analogous distances in α-CuBr at 485°C.

Description of the Structure Including Conduction Pathways

A projection of the Br^- and Py^+ ion structure down the *c*-axis of the unit cell of $Py_2Cu_5Br_7$ is shown in Fig. 1. As mentioned earlier, there

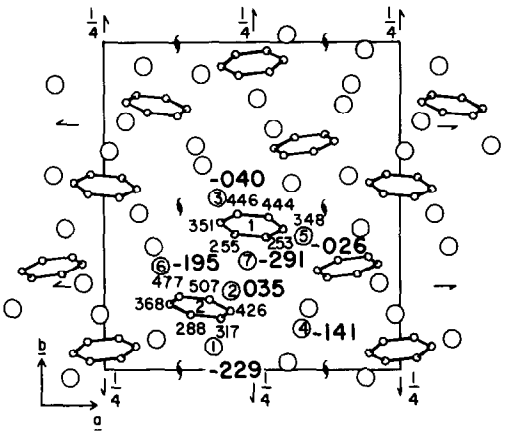

FIG. 1. [001] projection of the structure of $Py_2Cu_5Br_7$ excluding Cu^+ ions. The large circles represent Br^- ions; the small circles represent the atoms of the Py ring. The *z* values ($\times 10^3$) of the atoms in the asymmetric unit are indicated.

are seven independent Br^- ions in the asymmetric unit forming a pentagonal bipyramid. A pentagonal bipyramid is actually a part of a centered icosahedron (Fig. 2), parts or all of which occur in structures of solid electrolytes based on silver iodide. Each bipyramid has Br2 and Br7 as the apices lying on the approximate fivefold axis and Br1,2,4,5,6 as the apices of the approximate pentagon (Fig. 2). There are four such bipyramids in the unit cell. Each bipyramid contains five tetrahedra which share the edge connecting Br2 and Br7; the tetrahedral sites for the Cu^+ ions in the bipyramids are labeled 1, 5, 6, 10, and 11 (Table III). Neighboring bipyramids are connected by tetrahedra formed by Br^- ions belonging to different bipyramids.

The connections between the bipyramids occur in two ways, each involving the formation of four independent tetrahedra. One

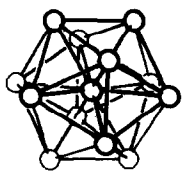

FIG. 2. The relation of a pentagonal bipyramid (idealized) to the regular icosahedron.

TABLE III

BROMIDE TETRAHEDRA ABOUT THE Cu^+ ION SITES

Site	Fractional occupancy	Br–Br[a] (Å)				Av Br–Br (Å)	Cu–Br (Å)				Av Cu–Br (Å)	No. of Cu neighbors	Cu–Cu (Å)		Av Cu–Cu (Å)	Volume (Å³)
Cu1	0.80	1–2[b]	3.987	2–4	4.068	4.081	Br1	2.43	Br4	2.49	2.51	3	Cu2	1.55	1.69	7.87
		1–4	4.123	2–7	4.113		Br2	2.69	Br7	2.41			Cu6	1.73		
		1–7	4.036	4–7	4.158								Cu10	1.78		
Cu2	0.11	1–3	4.310	3–4	4.073	4.296	Br1	2.45	Br4	2.40	2.63	2	Cu1	1.55	1.66	8.86
		1–4	4.123	3–7	5.077		Br3	2.88	Br7	2.80			Cu3	1.77		
		1–7	4.036	4–7	4.158											
Cu3	0.14	1–3	4.310	3–4	4.073	4.206	Br1	2.46	Br4	2.66	2.58	3	Cu2	1.77	1.73	8.52
		1–4	4.123	3–7	4.215		Br3	2.55	Br7	2.64			Cu4	1.70		
		1–7	3.888	4–7	4.629								Cu13	1.72		
Cu4	0.70	1–3	4.310	3–5	4.160	4.073	Br1	2.61	Br5	2.44	2.51	2	Cu3	1.70	1.55	7.84
		1–5	3.735	3–7	4.215		Br3	2.49	Br7	2.49			Cu5	1.40		
		1–7	3.888	5–7	4.130											
Cu5	0.13	2–3	4.136	3–5	4.160	4.133	Br2	2.49	Br5	2.50	2.53	3	Cu4	1.40	1.68	8.70
		2–5	4.042	3–7	4.215		Br3	2.57	Br7	2.56			Cu6	1.70		
		2–7	4.113	5–7	4.130								Cu11	1.93		
Cu6	0.10	2–4	4.068	4–5	4.174	4.114	Br2	2.48	Br5	2.51	2.52	3	Cu1	1.73	1.66	8.20
		2–5	4.042	4–7	4.158		Br4	2.55	Br7	2.55			Cu5	1.70		
		2–7	4.113	5–7	4.130								Cu7	1.54		
Cu7	0.89	2–4	4.068	4–5	4.174	4.061	Br2	2.54	Br5	2.47	2.49	2	Cu6	1.54	1.57	7.88
		2–5	4.042	4–6	4.057		Br4	2.39	Br6	2.57			Cu8	1.59		
		2–6	3.981	5–6	4.046											
Cu8	0.07	2–4	4.122	4–5	4.174	4.094	Br2	2.50	Br5	2.46	2.51	3	Cu7	1.59	1.65	8.65
		2–5	3.903	4–6	4.057		Br4	2.53	Br6	2.54			Cu9	1.70		
		2–6	4.263	5–6	4.046								Cu12	1.65		
Cu9	0.81	1–2	3.987	2–5	3.903	4.051	Br1	2.42	Br5	2.49	2.49	2	Cu8	1.70	1.61	8.23
		1–5	3.943	2–6	4.263		Br2	2.52	Br6	2.51			Cu10	1.51		
		1–6	4.161	5–6	4.046											

Cu10	0.18	1–2	3.987	2–6	4.263	4.095	Br1	2.49	Br6	2.56	2.51	3	Cu1	1.78	1.74	8.06
		1–6	4.161	2–7	4.113		Br2	2.54	Br7	2.45			Cu9	1.51		
		1–7	4.036	6–7	4.012								Cu11	1.94		
Cu11	0.70	2–3	4.136	3–6	4.279	4.170	Br2	2.70	Br6	2.41	2.58	4	Cu5	1.93	1.74	8.51
		2–6	4.263	3–7	4.215		Br3	2.39	Br7	2.82			Cu10	1.94		
		2–7	4.113	6–7	4.012								Cu12	1.34		
													Cu13	1.73		
Cu12	0.28	2–3	4.136	3–4	4.107	4.161	Br2	2.56	Br4	2.47	2.55	2	Cu8	1.65	1.50	8.46
		2–4	4.122	3–6	4.279		Br3	2.56	Br6	2.60			Cu11	1.34		
		2–6	4.263	4–6	4.057											
Cu13	0.10	3–4	4.073	4–6	5.124	4.389	Br3	2.42	Br6	2.81	2.69	2	Cu3	1.72	1.73	9.43
		3–6	4.279	4–7	4.629		Br4	2.96	Br7	2.57			Cu11	1.73		
		3–7	4.215	6–7	4.012											

[a] There is one Br3–Br6 distance of 4.751(9) Å that is not an edge of a tetrahedron.
[b] The designation 1–2, for example, denotes the Br1–Br2 distance.

TABLE IV

CORDINATIONS OF THE Br^- IONS AND AVERAGE DISTANCES IN ÅNGSTROMS

Bromide designation	No. of Br^- neighbors	Average[a] Br/Br distance (Å)
Br1	8	4.023
Br2	9	4.068
Br3	9	4.335
Br4	10	4.264
Br5	8	4.016
Br6	9	4.297
Br7	9	4.251

[a] See Table II for individual Br–Br distances. The standard error of all average distances is 0.009 Å.

yields the Cu^+ ion sites 7, 8, 9, and 12, the group labeled *G*; the second yields Cu^+ ion sites 2, 3, 4, and 13, the group labeled *Γ*. Thus there are 13 independent Cu^+ ion tetrahedral sites and therefore a total of 52 such sites in the unit cell.

Figure 3 shows the arrangement of the pentagonal bipyramids (denoted by BP) and the groups of connecting tetrahedra G and *Γ*. The four *equivalent* bypyramids are numbered 1, 2, 3, 4 for ease of discussion. The symbol $2_1(x,\frac{1}{4},0)$ (and analogous symbols) is intro-

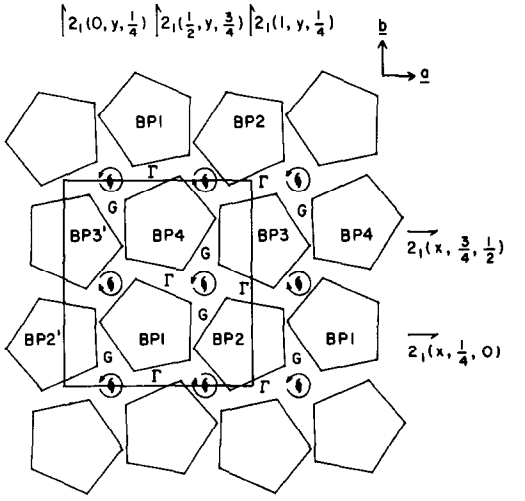

FIG. 3. Arrangement of the pentagonal bipyramids and *G* and *Γ* groups of bromide ion tetrahedra (see text).

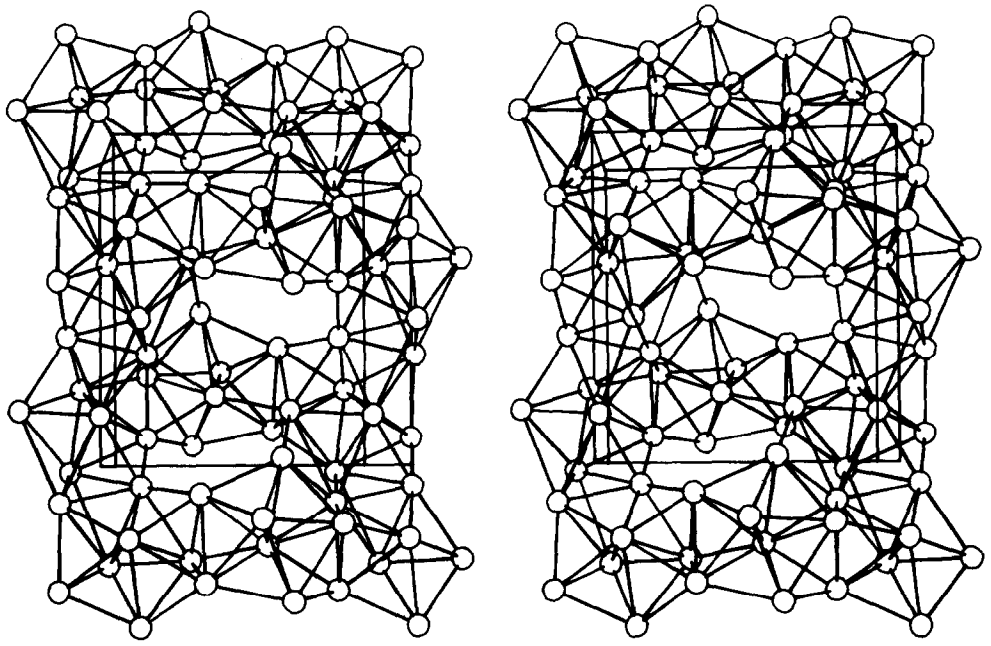

FIG. 4. Stereoscopic drawing of the Br^- ion arrangement in $Py_2Cu_3Br_7$, looking along the c-axis.

duced to denote a 2_1-axis along a at $y = \frac{1}{4}$, $z = 0$.

Conduction of Cu^+ ions in the [100] direction occurs via BP1 → G → BP2 → G → BP1 (in the next cell all along a) and so on. BP1 is transformed to BP2 by $2_1(x,\frac{1}{4},0)$. The channel thus runs along a, centered about $2_1(x,\frac{1}{4},0)$, in an undulating fashion, the amplitude[8] in the c-direction being $z = \pm 0.128$.

The $2_1(\frac{3}{4},\frac{1}{2},z)$ axis transforms BP1 into BP3 and BP2 into BP4; therefore the channel BP4 → G → BP3 → G → BP4 (in the next unit cell along a) ... centred about $2_1(x,\frac{3}{4},\frac{1}{2})$ is also along the a-direction and is entirely equivalent to that centered about $2_1(x,\frac{1}{4},0)$ (Fig. 3). Along the b-direction, BP2 is connected to BP3 via Γ, again forming an undulating channel: BP2 → Γ → BP3 → Γ → Γ → BP2 (in the next unit cell along b) ... centered about $2_1(1,y,\frac{1}{4})$; the amplitude of this channel in the c-direction is $z = \pm 0.122$. The $2_1(1,y,\frac{1}{4})$ (Fig. 3) axis transforms BP2 into BP3. The $2_1(\frac{3}{4},\frac{1}{2},x)$ axis transforms the whole channel centered at $2_1(1,y,\frac{1}{4})$ into the channel centered at $2_1(\frac{1}{2},y,\frac{3}{4})$. As indicated earlier, the two channels are entirely equivalent; however, the designation (Fig. 3) is now BP1 (next unit cell along b) → Γ → BP4 → Γ → BP1 ....

The stereoscopic drawing (Fig. 4) looking down the c-axis shows the conduction passageways along a and b. Figures 3 and 4 show that the channels in the a-direction are interconnected, as are the channels in the b-direction. Moreover, the channels in the a- and b-directions are interconnected. There is zero *average* change in the c-direction when a Cu^+ ion moves along a *single* channel in either the a- or b-direction. However, a net change occurs along c when the Cu^+ ion moves from one channel to another.

The above description does not yet distinguish the most probable individual pathways in the crystal. These are obtained by a more detailed examination of Table III, which gives the interconnections of Cu^+ ion sites and the site occupancies. There is no obvious reason for the observed distribution which is mar-

[8] The amplitude is defined as the perpendicular distance of the midpoint between Br2 and Br7 to the appropriate 2_1-axis, in this *particular* case, $2_1(x,\frac{1}{4},0)$.

kedly nonuniform, as might be expected from the results of the studies of the AgI-based solid electrolytes (*1–9*). It should be clear, however, that the total fractional occupancy of two adjacent sites must be $\leqslant 1.0$. The equivalent to high fractional occupancy is high residence time. High residence time means that the contribution of the ions in such sites to the average mobility in a particular direction, is lower than for ions in less populated sites.[9]

The detailed pathways along *a* and *b* are shown schematically in Fig. 5. Along *a*, the most probable path is 6 → 7 → 8 → 12 → 11 → 5 → 6 .... This path includes two highly occupied sites, Cu7 and Cu11, per increment. The alternate path 6 → 7 → 8 → 9 → 10 → 1 → 6 ... includes three highly occupied sites per increment, namely, Cu7, Cu9, and Cu1. Along

[9] It should be mentioned here that the application of an electric field to the crystal could conceivably change the equilibrium distribution that exists in the unperturbed crystal.

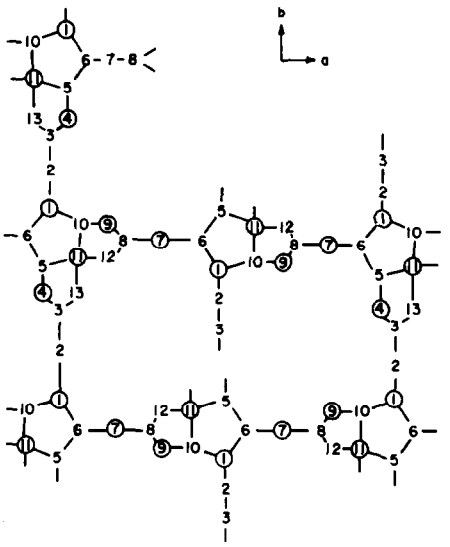

FIG. 5. Schematic representation of conduction pathways in *a*- and *b*-directions. The numbers denote Cu^+ ion sites as in Table III. Circled numbers indicate fractional occupancy $\geqslant 0.70$.

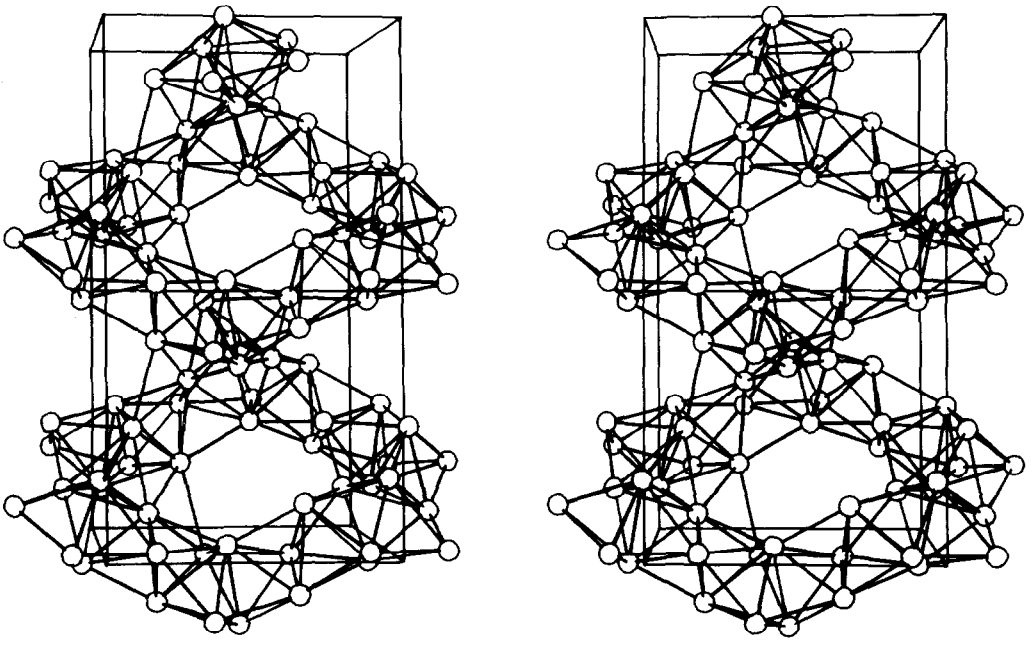

FIG. 6. Stereoscopic drawing of the Br^- ion arrangement in $Py_2Cu_5Br_7$, looking along *b*. Two unit cells along *c* are shown.

b, two paths appear to be about equally probable; these are $1 \rightarrow 2 \rightarrow 3 \rightarrow 4 \rightarrow 5 \rightarrow 6 \rightarrow 1$ ... and $1 \rightarrow 2 \rightarrow 3 \rightarrow 13 \rightarrow 11 \rightarrow 10 \rightarrow 1$ .... Each increment contains two highly occupied sites.

The sites in the pentagonal bipyramids connect channels along a and b, but groups G and Γ are strictly in the a and b channels, respectively.

An electric field in the c-direction must result in a *net* drift of Cu^+ ions in this direction. The two most efficient pathways which allow motion of the Cu^+ ions effectively in the c-direction are right- and left-handed helical paths. The right-handed path is BP1 $\rightarrow$ G $\rightarrow$ BP2 $\rightarrow \Gamma \rightarrow$ BP3 $\rightarrow$ G $\rightarrow$ BP4 $\rightarrow \Gamma \rightarrow$ BP1 (in the next cell along c) $\rightarrow$ ...; the spiral is about the $2_1(\frac{3}{4}, \frac{1}{2}, z)$ axis. The left-handed helical path is BP1 $\rightarrow$ G $\rightarrow$ BP2′ (i.e., in the next unit cell along $-b$) $\rightarrow \Gamma \rightarrow$ BP3′ $\rightarrow$ G $\rightarrow$ BP4 $\rightarrow \Gamma \rightarrow$ BP1 (in the next unit cell along c) $\rightarrow$ ...; the spiral is about the $2_1(\frac{1}{4}, \frac{1}{2}, z)$ axis. Figure 3 shows how the network of helical paths is arranged. The symbols ◯ and ◯ denote right- and left-handed rotation, respectively, of the helical paths in the (positive) c-axis direction. Each helical path is surrounded by four nearest-neighbor helical paths with opposite

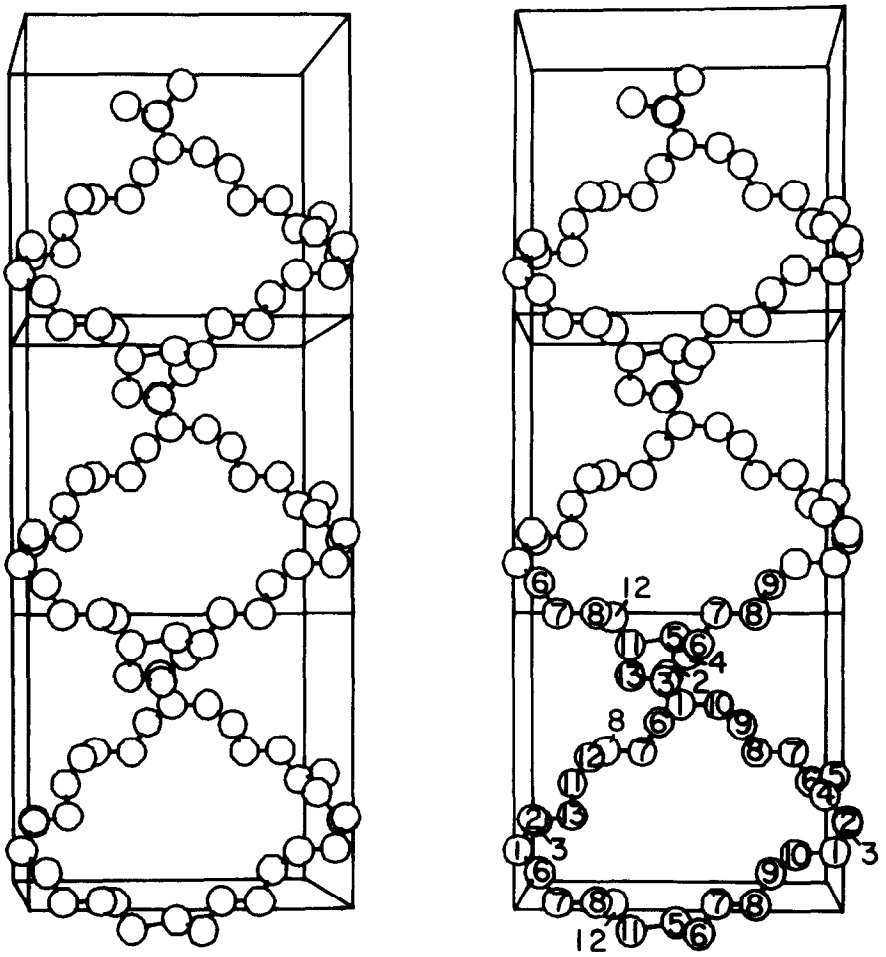

FIG. 7. Stereoscopic drawings of the conduction paths of the Cu^+ ions, looking along b. The numbers correspond to those listed in Table I. Three unit cells along the c-axis are shown.

chirality and four next-nearest-neighbor helical paths with the same chirality. In a single turn, a particular helix shares four bipyramids (BP's) with these eight neighbors, and 2 *G*'s and 2 *I*'s with the four nearest neighbors.

The stereoscopic drawing shown in Fig. 6 illustrates the Br^- ion tetrahedra forming the two spirals of different chirality. These spirals are the only paths that will allow Cu^+ ions to move in the *c*-direction. Figure 7 is a stereoscopic drawing depicting the "spiral routes" by means of the equilibrium Cu^+ ion sites only. The most effective routes, in terms of Cu^+ ion site designations, are: right-handed, 5 → 6 → 7 → 8 → 9 → 10 → 1 → 2 → 3 → 4 → 5 ...; left-handed, 11 → 12 → 8 → 7 → 6 → 1 → 2 → 3 → 13 → 11 . . .. Of these the more probable is the latter; it contains 9 as opposed to 10 sites per increment and three as opposed to four highly occupied sites per increment of the former.

The stereoscopic drawing in Fig. 8 shows the surroundings of the Py^+ rings. The rings in each pair (Py1 and Py2) are approximately parallel (a *small* resemblance to the arrangement in PyCl (*35*)). Py1 is approximately parallel to the (distorted) hexagon of Br^- ions, 2, 5, 1, 5, 3, 6 nearby; Py2 is at an angle to the symmetry-related Br^- ion hexagon nearby. Py1 has 13 Br^- ion near neighbors and Py2 has 12 Br^- ion near neighbors. Although C and N have not been distinguished in the refinement, the best candidates for the N atom are *C*1 of Py1 and *A*2 of Py2, because of the particular way the Br^- ions surrounding the Py^+ ions are arranged (see also Ref. (*3*)).

Further Discussion

The average conductivity of $Py_2Cu_5Br_7$ reported by Skarstad and Parker (*18*) is 0.017 $(\Omega\ \text{cm})^{-1}$ at 292°K. We intend to measure the directional conductivity of $Py_2Cu_5Br_7$.[10] We can predict from the observations given above that the conductivity in the *b*-direction will be *somewhat* higher than that in the *a*-direction, and that the conductivity in the *c*-direction will be *substantially* lower than that in the *a*-direction.

The total number of Cu^+ ion sites in the unit cell is 52; the total number of Cu^+ ions in the unit cell is 20, giving a ratio of 2.6 available sites per mobile carrier. This is even lower than the lowest for any of the AgI-based solid electrolytes of which the structures have been determined. The lowest is 3.06 for $Py_5Ag_{18}I_{23}$ (*7*, *9*). The average conductivity, 0.008 (*3*) or

[10] Some time will elapse before we have the required crystals which we intend to grow by the Czochralski technique (*18*).

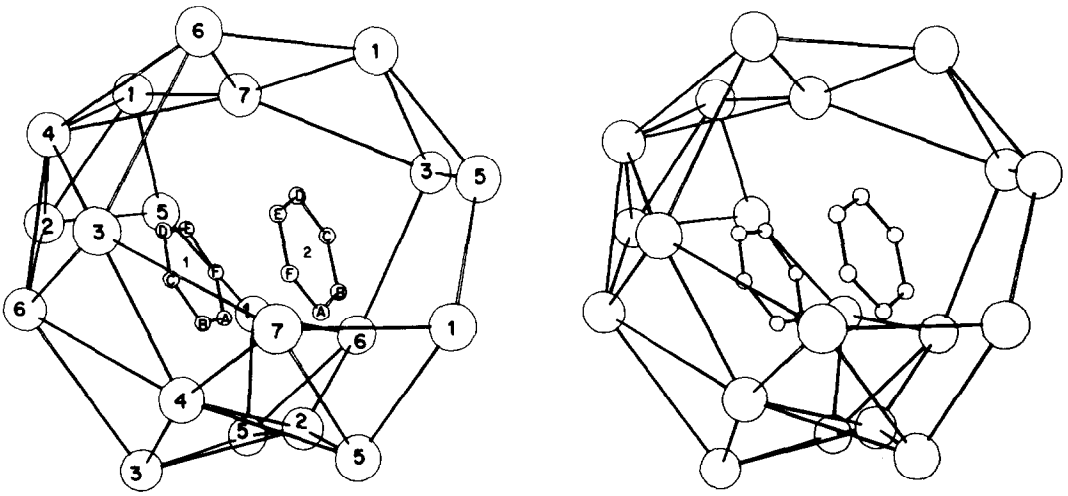

FIG. 8. Stereoscopic drawing showing Br^- ion arrangement about two independent Py^+ ions in $Py_2Cu_5Br_7$.

0.011 (*11*) $(\Omega\ cm)^{-1}$, of $Py_5Ag_{18}I_{23}$ is comparable with that of $Py_2Cu_5Br_7$, but that of the former is lower, probably mainly because it is only a two-dimensional solid electrolyte.

The volumes of the Br^- tetrahedra calculated by assuming the individual tetrahedron to be formed by the positions of the Br nucleii are listed in Table III. The total volume occupied by the Br^- ion tetrahedra per unit cell is 436.8 Å^3, which is only 20.2% of the unit cell volume. This is very low relative to the lowest observed, 31.6%, again that of $Py_5Ag_{18}I_{23}$. This result could also support the thesis that a three-dimensional solid electrolyte is apt to be better than a two-dimensional one, even when the other parameters are not as favorable. The carrier concentrations of $Py_2Cu_5Br_7$ and $Py_5Ag_{18}I_{23}$ (*7*, *9*) are 0.92 and 0.89 $\times$ 10^{22}, respectively, and the site concentrations are 2.40 and 2.72 $\times$ 10^{22}, respectively.

Acknowledgment

We thank Dr. C. G. Pierpont and Mr. R. C. Haltiwanger of the Chemistry Department of the University of Colorado, Boulder, Colorado, for their help with the computer programs used in this work.

References

1. S. GELLER, *Science* **157**, 310 (1967); S. GELLER AND M. D. LIND, *J. Chem. Phys.* **52**, 5854 (1970); S. GELLER, *Phys. Rev. B* **14**, 4345 (1976).
2. S. GELLER, *Science* **176**, 1016 (1972); S. GELLER AND B. B. OWENS, *J. Phys. Chem. Solids* **33**, 1241 (1972).
3. S. GELLER AND P. M. SKARSTAD, *Phys. Rev. Lett.* **33**, 1484 (1974); S. GELLER, P. M. SKARSTAD, AND S. A. WILBER, *J. Electrochem. Soc.* **122**, 332 (1975).
4. L. Y. Y. CHAN AND S. GELLER, *J. Solid State Chem.* **21**, 331 (1977).
5. H. WIEDERSICH AND S. GELLER, *in* "The Chemistry of Extended Defects in Non-Metallic Solids" (L. Eyring and M. O'Keeffe, Eds.), pp. 629–650, North–Holland, Amsterdam (1970).
6. S. GELLER, *in* "Fast Ion Transport in Solids" (W. van Gool, Ed.), pp. 607–616, North–Holland/American Elsevier, Amsterdam/New York (1973).
7. S. GELLER, *in* "Superionic Conductors" (G. D. Mahan and W. L. Roth, Eds.), pp. 171–182, Plenum, New York/London (1976).
8. S. GELLER, *Accounts Chem. Res.*, in press.
9. S. GELLER, *in* "Solid Electrolytes" (S. Geller, Ed.), pp. 41–66, Springer–Verlag, Heidelberg (1977).
10. K. FUNKE, *Progr. Solid State Chem.* **11**, 345 (1976).
11. T. HIBMA, *Phys. Rev. B* **15**, 5797 (1977); W. J. PARDEE AND G. D. MAHAN, *J. Solid State Chem.* **15**, 310 (1975).
12. B. B. OWENS, *in* "Advances in Electrochemistry and Electrochemical Engineering" (C. W. Tobias, Ed.), Vol. 8, pp. 1–62, Wiley, New York (1970); B. B. OWENS AND G. R. ARGUE, *J. Electrochem. Soc.* **117**, 898 (1970), *Science* **157**, 308 (1967); B. B. OWENS, *J. Electrochem. Soc.* **117**, 1536 (1970); B. B. OWENS, *in* "Fast Ion Transport in Solids" (W. van Gool, Ed.), pp. 593–606, North–Holland/American Elsevier, Amsterdam/New York (1973); B. B. OWENS, J. H. CHRISTIE, AND G. T. TIEDEMAN, *J. Electrochem. Soc.* **118**, 1144 (1971); J. H. CHRISTIE, B. B. OWENS, AND G. T. TIEDEMAN, *Inorg. Chem.* **14**, 1423 (1975).
13. B. REUTER AND K. HARDEL, *Naturwissenschaften* **48**, 161 (1961); *Anorg. Allg. Chem.* **340**, 158, 168 (1965); *Ber. Bunsenges. Phys. Chem.* **70**, 82 (1966).
14. M. L. BERARDELLI, C. BIONDI, M. DEROSSI, G. FONSECA, AND M. GIOMINI, *J. Electrochem. Soc.* **119**, 114 (1974).
15. T. TAKAHASHI, S. IKEDA, AND O. YAMAMOTO, *J. Electrochem. Soc.* **119**, 477 (1972); **120**, 647 (1973).
16. J. COETZER AND M. THACKERAY, *Electrochim. Acta* **21**, 37 (1976).
17. A. F. SAMMELLS, J. Z. GOUGOUTAS, AND B. B. OWENS, *J. Electrochem. Soc.* **122**, 1291 (1975).
18. P. M. SKARSTAD AND H. S. PARKER, *J. Crys. Growth*, in press.
19. P. B. CRANDALL, *Rev. Sci. Instrum.* **41**, 1895 (1970).
20. A. SCHUYFF AND J. B. HULSCHER, *Rev. Sci. Instrum.* **36**, 957 (1968).
21. FAMEB is a modified version of FAME by R. B. K. DEWAR.
22. MULTANB is a modified version of MULTAN by P. MAIN, M. M. WOOLFSON, AND G. GERMAIN.
23. FORDAPB is a modified version of FORDAP by A. ZALKIN.
24. NUCLS 5 is a highly modified version by J. A. IBERS AND R. J. DOEDENS of ORFLS by W. R. BUSING, K. O. MARTIN, AND H. A. LEVY, Oak Ridge National Lab. Report ORNL-TM-305 (1962).
25. H. HARTL, *Acta Crystallogr. B* **31**, 1781 (1975).

26. D. T. CROMER AND D. LIBERMAN, *J. Chem. Phys.* **53**, 1891 (1970).
27. D. T. CROMER AND J. B. MANN, *Acta Crystallogr. A* **24**, 321 (1968).
28. ORRFEC is a modified version by J. A. IBERS of the Oak Ridge ORFFE 3 program version of January 1971.
29. C. K. JOHNSON, Oak Ridge National Lab. Report ORNL-3794, rev. (1965).
30. S. HOSHINO, *J. Phys. Soc. Japan* **7**, 560 (1952).
31. W. BÜHRER AND W. HÄLG, *Electrochim. Acta* **22**, 701 (1977).
32. J. KRUG AND L. SIEG, *Z. Naturforsch. A* **7**, 369 (1952).
33. C. TUBANDT, *in* "Handbuch der Experimentalphysik," Vol. XII, Part I, p. 447, Akad. Verlagsgesellschaft, Leipzig (1932).
34. H. E. SWANSON, R. K. FUYAT, AND G. M. UGRINIC, *Nat. Bur. Std. (USA)* Circ. **359**, 4, 36 (1955).
35. C. RÉRAT, *Acta Crystallogr.* **15**, 427 (1962).